

Fishbone Instability Triggered Nonlocal Transient Transport in HL-2A NBI Plasmas

W. Chen¹, Y. Xu¹, X.T. Ding¹, Z.B. Shi¹, M. Jiang¹, W.L. Zhong¹, X.Q. Ji¹, D.L. Yu¹, Z. C. Yang¹, L.M. Yu¹, J.X. Li¹, Y. G. Li¹, J.Y. Cao¹, X.M. Song¹, M. Xu¹, L.W. Yan¹, Yi. Liu¹, Q.W. Yang¹, and X.R. Duan¹

¹ *Southwestern Institute of Physics, P.O. Box 432 Chengdu 610041, China*

A new-type nonlocal transient transport[1][2] induced by the fishbone instability has been observed in HL-2A ($R/a = 1.65m/0.4m$) low-density ($ne < 1.5 \times 10^{19} m^{-3}$) NBI plasmas with the lower single-null divertor configuration. This phenomenon is well reproducible. Figure 1 shows typical experimental results with the fishbone instability and nonlocal transport during NBI. The sawteeth are gradually suppressed by beam ions after the NBI is switched on at $t = 410ms$. The fishbones with bursting-amplitude and chirping-frequency are driven by energetic ions during $t = 550 - 650ms$. The repetitive fishbones produce the similar effect like the modulated heating/cooling pulses. The lifetime of each fishbone is $t_f = 3 - 5ms$, and the interval-time of two fishbones is $\Delta t = 3 - 7ms$. The deuterium-alpha radiation (D_α) in the divertor drops significantly while the fishbone bursts, and the line-averaged density does hardly change.

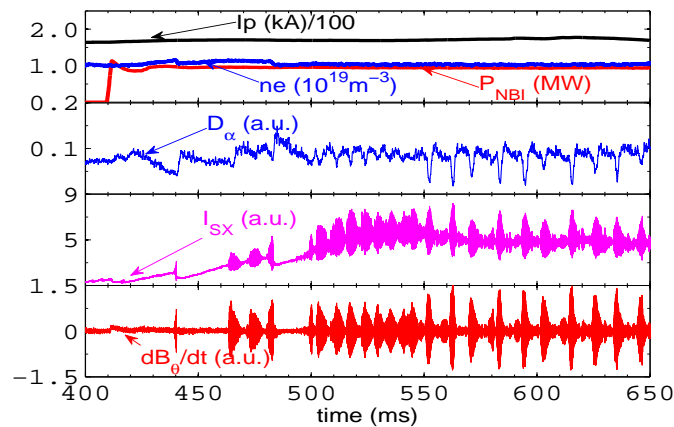


Figure 1: Typical discharge with fishbone (fb) instability and nonlocal phenomenon on HL-2A. Plasma current, Ip ; electron density, ne ; NBI power, P_{NBI} ; deuterium-alpha radiation in the divertor, D_α ; soft X-ray signal in the core, I_{SX} ; Mirnov signal in the midplane, dB_θ/dt .

The radial localization and fluctuation amplitudes of the $m/n=1/1$ fishbone are measured by the multi-channel ECE radiometer. Figures 2(a-d) show spectrograms of autopower of ECE signals at radial positions $\rho = 0.07$, $\rho = 0.15$, $\rho = 0.23$ and $\rho = 0.30$. Furthermore, the fishbones do not occur at spectrograms of autopower of ECE signals in the region of $\rho \geq 0.30$, but appear at spectrograms of crosspower of Mirnov data and ECE signals. Therefore it is inferred that

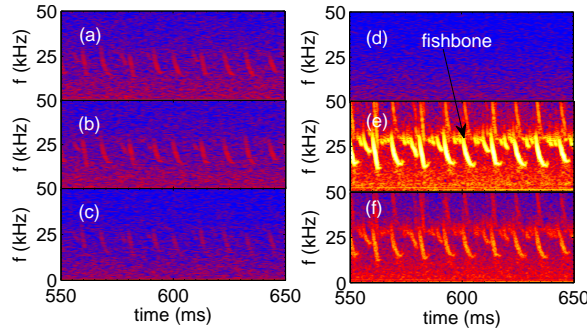


Figure 2: Spectrograms (a-d) of autopower of ECE signals at different radial positions, (a) $\rho = 0.07$, $\rho = 0.15$, $\rho = 0.23$ and $\rho = 0.30$; spectrogram (e) of autopower of the Mirnov signal; spectrogram (f) of crosspower of Mirnov data and ECE signal at $\rho = 0.30$. Spectrograms of autopower of ECE signals and spectrograms of crosspower of Mirnov data and ECE signals are similar and not shown here while $\rho > 0.3$

the fishbones localize in the core, $\rho < 0.30$, and the fishbone-induced temperature perturbation spreads to the plasma edge. The traces of electron temperatures are shown in Figure 3. With the fishbone bursting it is found that the core (localization of fishbone, $\rho < 0.30$) heating leads to a simultaneous decrease (but not slow increase) in temperature at the plasma edge. The reversal radius of temperatures is $\rho \simeq 0.55$, which is near $q=3/2$ rational surface. The effect reveals fast anomalous transport of core heat pulses to plasma edge, not compatible with diffusive time scales. It is a new-type nonlocal response which is a counterpart to that induced by the edge heating/cooling pulse. The perturbation source of the new-type nonlocal is magnetic, and it is produced by the plasma itself.

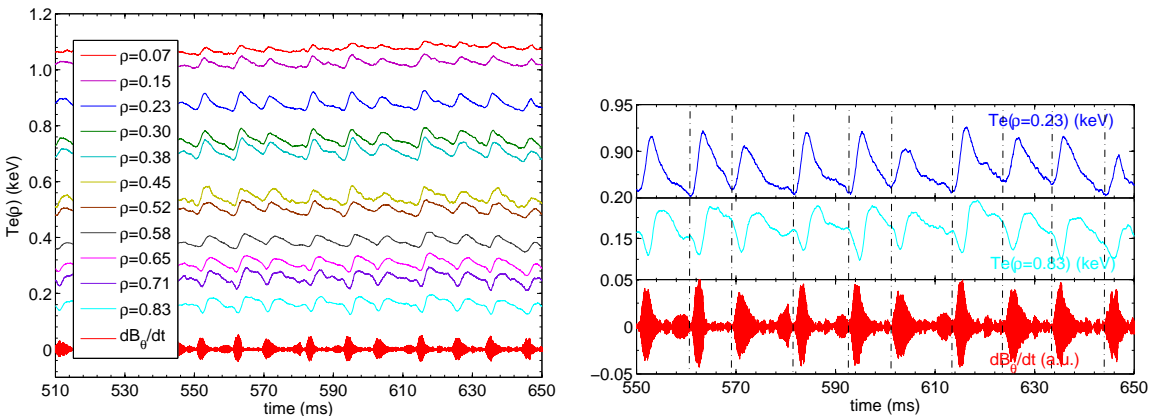


Figure 3: Time evolution of the Mirnov signal (dB_θ/dt) with strong ion fishbone instabilities and electron temperatures (T_e) at different radial positions. Panoramic view (left) and local view (right).

A novel result, the nonlinear coupling between the fishbone and background turbulence during the nonlocal, has been analyzed by the bispectrum technique. The squared bicoherence is given by $\hat{b}^2(f_1, f_2) = |\hat{B}_{Te\tilde{B}_\theta\tilde{B}_\theta}(f_1, f_2)| / <|Te(f_1)\tilde{B}_\theta(f_2)|^2><|\tilde{B}_\theta(f_3)|^2>$ with the Fourier bispectral $\hat{B}_{Te\tilde{B}_\theta\tilde{B}_\theta}(f_1, f_2) = <Te(f_1)\tilde{B}_\theta(f_2)\tilde{B}_\theta^*(f_3)>$, $f_3 = f_1 \pm f_2$ and $0 < \hat{b}^2(f_1, f_2) < 1$. The squared-bicoherences of magnetic and temperature fluctuations are shown in Figure 4. It is found that $|f_2| = k * f_{fb}$ and $|f_2 \pm f_1| = k * f_{fb}$ (k is a positive integer) are strong coupling lines. It indicates that the nonlinear interaction between the fishbone and background turbulence and there exists energy transfer between fishbone and temperature fluctuations. This may explain why the core ($\rho < 0.3$) electron temperature increases abnormally while the fishbone bursts. It also suggests that the multi-scale (macro-transport, meso-EP/MHD and micro-turbulence) physics is responsible for the global nonlocal response.

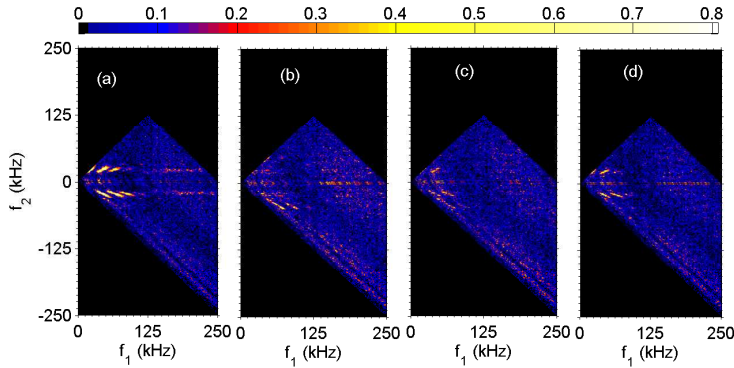


Figure 4: Squared bicoherences (a-d) $\hat{b}^2_{Te\tilde{B}_\theta\tilde{B}_\theta}(f_1, f_2)$ at different radial positions. (a) $\rho = 0.23$, (b) $\rho = 0.38$, (c) $\rho = 0.52$, and (d) $\rho = 0.65$.

Figure 5 shows the auto-correlation function (ACF) coefficients (a-b) of ECE signals at two radial positions ($\rho = 0.23 < \rho_{rev}$ and $\rho = 0.65 > \rho_{rev}$) and spatial profiles (c) of Hurst exponents (H , obtained by R/S method) from ECE signals. It is found that ACFs and Hurst exponent both enhances during the fishbone and nonlocal transport. And so the new-type nonlocal transport is potentially linked to self-organized critical (SOC) dynamics. Figure 5(d) gives that 2D pattern (d) of cross-correlation coefficients from ECE signals. It shows that the fluctuations induced by the fishbone is a long-range correlation, and the local micro-fluctuations communicate with those at distant radius via the long-range correlation, and the heat energy with $f = 20 - 22\text{kHz}$, which is the power-spectral peak of the fishbone, rapidly propagates outward. Meanwhile, it is observed that there are two phase jumps near the $q=1$ ($0.2 < \rho < 0.3$) and $q=3/2$ ($0.5 < \rho < 0.6$) rational surfaces. The phase jump is likely due to the presence of the shear flow which alters the mode propagation. It is found from figure 5(d) that the response time of the nonlocal transport is around $\tau \simeq 50\mu\text{s}$ in the radial distance, $0 < \rho < 0.8$, and the velocity of the radial propagation

is $v_r \simeq 0.8a/\tau \simeq 6\text{km/s}$.

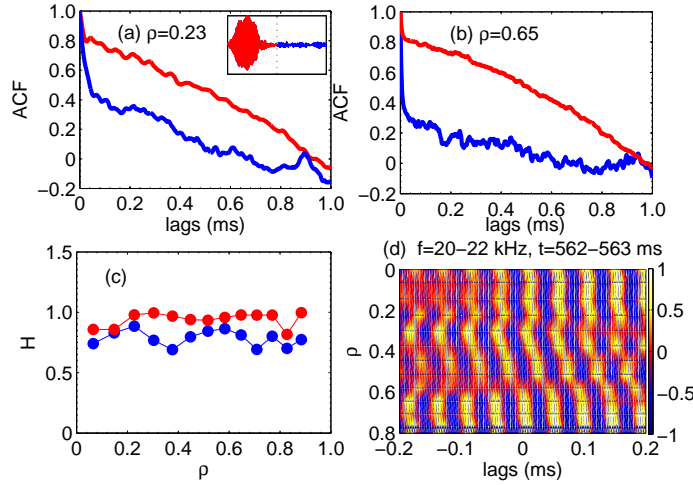


Figure 5: Auto-correlation function (ACF) coefficients (a-b) of ECE signals at two radial positions; Spatial profiles (c) of Hurst exponents (H) from ECE signals; 2D pattern (d) of cross-correlation coefficients from ECE signals. Red line with fishbone, blue line without fishbone. ACFs are similar and not shown here at other positions.

In summary, an experimental observation of a new-type nonlocal transport, which is triggered by the ion fishbone instability, is presented in a laboratory plasma. The rapid core heating leads to a simultaneous decrease in temperature in the plasma edge. The effect reveals anomalously fast transport of core heat pulses to plasma edge, not compatible with diffusive time scales. These results prove clearly that the magnetic perturbation, long-range correlation, meso-scale structure as well as $E \times B$ flow play crucial roles in the nonlocal response, and demonstrate explicitly that the fast response ($\sim 100\mu\text{s}$) of the nonlocal is electromagnetic but not electrostatic. The experimental results suggest there is a complexity coupling between the strong fishbone excitation and fluctuation-induced transport. The nonlinear coupling induces the energy transfer between the fishbone and background turbulence, and it is one of mechanisms of the fishbone-induced temperature increase in the core regions. The magnetic perturbation along with shear flow should dominate the nonlocal transient transport. The results also indicate that the nonlocal response is potentially linked to SOC dynamics.

This work is supported in part by the ITER-CN under Grants No. 2013GB104000 and 2013GB106004, and by the NNSF of China under Grant No. 11261140326, 11475058 and 11405049.

References

- [1] Callen, J.D. and Kissick, M.W. *Plasma Phys. Control. Fusion* **39**, B173-B188 (1997).
- [2] Ida, K. *et al. Nucl. Fusion* **55**, 013022 (2015).